European Journal of Business & Social Sciences
Available at https://ejbss.org/

ISSN: 2235-767X
Volume 07 Issue 05
May 2019

Thermal performance of artificially roughened solar air heater with booster mirror

PAWAR MAHESH RAJENDRA

ABSTRACT
Solar air heaters are one of the simplest and cost effective solar energy utilization systems for various drying applications. The thermal efficiency of solar air heaters is found to be low due to low heat transfer coefficient on the air side. Attempts have been made to enhance the heat transfer rate from the absorber plate to air by using different roughness elements. Enhancement of heat transfer coefficient is achieved by providing artificial roughness, always goes with an increment of pressure drop and more pumping power is required. So, there is a need to optimize the system parameters to maximize heat transfer, while keeping the friction losses as low as possible.
The present work aimed at obtaining the optimal thermo hydraulic performance condition in one sides roughened and glass covered solar air heaters to get the maximum heat transfer for minimum pumping power. An extensive experimental investigation has been carried out with the objective of obtaining and validating the results on heat transfer, friction factor, and thermal performance of one sides roughened and glass covered solar air heaters along with those on smooth and one sides glass covered solar air heaters. Roughened absorber plates were prepared by soldering small diameter wires on them. The operating parameters covered the range of relative roughness height, e/D, 8.35 × 10 -3 – 3.75 × 10 -2 , relative roughness pitch, p/e, 10 – 30, flow Reynolds number, Re, 4000 – 20000 and Prandtl number, P r , 0.7 for air. Data were collected on a similar sized one sides glass covered smooth solar air heater simultaneously. Calibrated copper constantan thermocouples were soldered on the absorber plates to measure local plate temperature, whereas, the temperature of air was measured by digital thermometer inserted midway into the air duct. Air was sucked through the collectors using a blower with electric power input controlled by an auto-variac to obtain variable flow rates, the flow rate being measured by a U-tube manometer fitted in a calibrated flange-tap orifice-meter.
Heat transfer measurements were conducted for a fully developed turbulent flow in a rectangular plate with its bottom wall blindly holed with circular geometry. The test plate was designed with its bottom wall was made of a rectangular GI plate of length 850 mm , breadth 100 mm and width150 mm. Experiments were carried out based on different geometries. It was found that the enhancement in heat transfer was achieved in

ISSN: 2235-767X
Volume 07 Issue 05
May 2019

rectangular plate with roughened on bottom surface of plate. Roughened on bottom of the GI plate enhance the convective heat transfer rate of the air flowing through it. Several experimental and numerical investigations, with different roughened geometry and flow conditions, have been carried out. This paper is one such effort of experimental investigations of heat transfer. It presents the effect of booster mirror arrangements on the heat transfer. This paper investigation on the thermal performance of artificially roughened solar air heater with booster mirror.

ACKNOWLEDGMENT

We would like to express our deep sense of gratitude to our guide Prof. Bhise Akash for his valuable guidance and motivation and for his extreme co-operation to complete the project work successfully. We would like to express our sincere respect and profound gratitude to Prof. Ingulkar Y.G. Head of Mechanical Engineering Department for supporting us and providing the facilities for the project work. We also thankful to DR. Walimbe Nihar Principal of Dhole Patil College Of Engineering for his continuous encouragement and guidance throughout the entire project work.

CHAPTER- 1

INTRODUCTION

Throughout the history of the human race, major developments have been accompanied by an increased consumption of energy. The degree of industrial advancement and prosperity of a nation is directly related to the per captain energy consumption of its people. More industrially developed countries consume more energy than developing and undeveloped countries. Those countries that have had abundant supply of energy available to them have substantially high rate of industrial growth and a corresponding high gross national product (GNP). The developing and developed countries have now to generate and harness more energy for their industrial growth and should be aware of conversion, conservation and development of new energy sources.

ISSN: 2235-767X
Volume 07 Issue 05
May 2019

A new and intense source of energy, nuclear energy came on the scene after the second world-war. The first large nuclear power station was commissioned in 1957 in the USA and nuclear energy has gained more momentum throughout the world. Energy consumption refers to the total energy used by all of human civilization. Typically measured per year, it involves all energy harnessed from every energy source applied towards humanity's endeavors across every industrial and technological sector, across every country. Being the power source metric of civilization, World Energy Consumption has deep implications for humanity's social-economic-political sphere. Two profound questions loom over all other energy concerns: Will we have enough affordable energy in the near future? What will we do for the long term?

The answers depend on our inventory of sources. At present, oil accounts for 40% of total energy consumption in the United States. Coal provides 23% and natural gas provides 22% of our energy. Another 8% comes from nuclear power plants. Renewable energy sources round out the roster, accounting for 7% of consumption – mostly as the result of hydropower investments made in the last century and the use of biomass (organic matter such as wood, municipal waste, and agricultural crops) for energy production. Those sources and their proportions will have to change eventually, since the planet's known supplies of fossil fuels are limited. But during the next couple of decades, the nation's energy menu is unlikely to be substantially different from todays – assuming “business as usual” conditions. Alternative energy is any energy source that is an alternative to fossil fuel. These alternatives are intended to address concerns about such fossil fuels. As conventional sources of energy are depleting at alarming rate.

1.1 Solar thermal collectors

A solar thermal collector collects heat by absorbing sunlight. A collector is a device for capturing solar radiation. Solar radiation is energy in the form of electromagnetic radiation from the infrared (long) to the ultraviolet (short) wavelengths. The quantity of

ISSN: 2235-767X
Volume 07 Issue 05
May 2019

solar energy striking the earth's surface (solar constant) averages about 1000 watts per square meter under clear skies, depending upon weather conditions, location and orientation. The term 'solar collector' commonly refers to solar hot water panels, but may refer to installations such as solar parabolic troughs and solar or basic installations such as solar air heaters. Concentrated solar power plants usually use the more complex collectors to generate electricity by heating a fluid to drive a turbine connected to an electrical generator. Simple collectors are typically used in residential and commercial buildings for space heating. Solar collectors are either non-concentrating or concentrating. In the non-concentrating type, the collector area (i.e., the area that intercepts the solar radiation) is the same as the absorber area (i.e., the area absorbing the radiation). In these types the whole solar panel absorbs light. Concentrating collectors have a bigger interceptor than absorber. Solar collectors, which are in use, are of two types:-

A. Flat plate collector

B. Concentrating collector

1.1.1 Flat plate collector

A flat-plate collector consists of an absorber, a transparent cover, a frame, and insulation. Usually an iron-poor solar safety glass is used as a transparent cover, as it transmits a great amount of the short-wave light spectrum. It is a simple device that is capable of collecting both direct & diffuse radiation. Their operating range includes temperature up to about 100^0C above ambient. Their low initial cost, simple construction and ease in maintenance has ma1de them easier for low temperature applications. Flat plate collectors are further categorized according to carrier fluid used as:-

(a) Liquid flat plate collector

(b) Air heating flat plat collector

ISSN: 2235-767X
Volume 07 Issue 05
May 2019

1.1.2 Concentrating collector

A solar collector that uses reflective surfaces to concentrate sunlight onto a small area, where it is absorbed and converted to heat or, in the case of solar photovoltaic (PV) devices, into electricity. Concentrators can increase the power flux of sunlight hundreds of times. The principle types of concentrating collectors include: compound parabolic, parabolic trough, fixed reflector moving receiver, fixed receiver moving reflector, Fresnel lens and central receiver. A PV concentrating module uses optical elements to increase the amount of sunlight incident onto a PV cell. Concentrating PV arrays track the sun and use concentrating devices to reflect direct sunlight onto the solar cell to produce electricity directly. Concentrating solar collectors in concentrated solar power facilities concentrate sunlight onto a receiver where it heats a heat transfer fluid that subsequently exchanges its absorbed heat to water to produce steam to power a steam turbine generator to produce electricity.

1.1.3 Solar air heaters

Solar air heaters are a system that collect solar energy and transfers the heat to passing air, which is either stored or used for space heating. The collectors are often black to absorb more of the sun's energy and a conductive material, often metal, acts as a heat exchanger. Solar air heaters can compliment traditional indoor heating systems by providing a free and clean source of heat.

1.2 PROBLEM STATEMENT

On the basis of above literature survey it can be concluded that all researchers have remained limited to only top side roughened collector having artificial roughness of different geometries which acts as the absorber plate and only top side glass covered which receives solar radiation and other one sides of the rectangular solar air heater duct having insulation, not receiving solar radiations and not booster mirror is used.

ISSN: 2235-767X
Volume 07 Issue 05
May 2019

1.3 OBJECTIVES OF THE PRESENT WORK

The present work has been taken up with the following objectives:

A. To analyze analytically the optimal thermo hydraulic performance of the onesides artificially roughened ducts for maximizing heat transfer while keeping friction loss minimum.
B. To perform experiments under actual outdoor conditions for data collection with respect to roughness and flow parameters.
C. To investigate the effect of artificial roughness introduced on the thermo hydraulic performance of one sides artificially roughened solar air heaters.

1.4 METHODOLOGY

The methodology taken for the current project is same as that of experimental setup developed by Prasad and Verma 2000 and Kumar Ashwini, 2017 for their thermal and themohydraulic performance for three sides artificial roughness geometries.

European Journal of Business & Social Sciences
Available at https://ejbss.org/
ISSN: 2235-767X
Volume 07 Issue 05
May 2019

CHAPTER- 2

LITERATURE REVIEW

Since the beginning of time, people have been fascinated by the sun. Ancient civilizations personified the sun, worshipping it as a God or Goddess. Throughout history, farming and agriculture efforts have relied upon the sun's rays to grow crops and sustain populations. Only recently, however, have we developed the ability to harness the sun's awesome power. The resulting technologies have promising implications for the future of renewable energy and sustainability.

2.1 COLLECTOR PERFORMANCE

The useful thermal energy for quasi-steady state condition, delivered by a solar collector is obtained from the energy balance between the energy absorption rate of the absorber & thermal energy losses directly and indirectly to the surroundings. It can be written as:

$$\frac{Q_u}{A_c} = I(\tau\alpha) - U_L(\overline{T}_p - T_a) \quad (2.1)$$

The difficulty is to utilize the above equation, which lies in the calculation of mean absorber plate temperature, $\overline{T}_p$, which is a function of the collector configuration, the incident solar radiation and entering fluid condition. Therefore, the Eq. (2.1) is usually represented in a more practical form as:

$$\frac{Q_u}{A_c} = F_R[I(\tau\alpha) - U_L(T_i - T_a)] \quad (2.2)$$

ISSN: 2235-767X
Volume 07 Issue 05
May 2019

where, the heat removal factor F_R is defined as the ratio of rate of actual useful energy collected to the rate if the entire collector surface were at fluid inlet temperature and can be written as:

$$F_R = \frac{\dot{m}C_P(T_o - T_i)}{A_c[I(\tau\alpha) - U_L(T_i - T_a)]} \quad (2.3)$$

A very widely used basic equation (2.2) known (Hottel-Whillier-Bliss equation) can be modified to include thermal efficiency as:

$$\eta_{th} = F_R\left[(\tau\alpha) - U_L\frac{(T_i - T_a)}{I}\right] \quad (2.4)$$

This equation expresses the thermal efficiency of the collector in terms of two major operating parameters, incidence solar radiation normal to the collector plate and temperature difference $(T_i - T_a)$.

Eqs. (2.2) and (2.4) have been in wide use to compare the performance characteristics of different types of collectors and to investigate the effect of various design parameters. Heat removal factor F_R is a function of plate efficiency factor F' defined by Bliss (1959), written under as:

$$F' = \frac{h}{h + U_L} \quad (2.5)$$

The value of F' is a strong function of configuration parameters given by (Duffie et al. 1980). A third factor known as collector flow factor F'' has been including (Duffie et al. 1980) to present equation as given below:

European Journal of Business & Social Sciences
Available at https://ejbss.org/
ISSN: 2235-767X
Volume 07 Issue 05
May 2019

$$F_R = \frac{\dot{m}C_P}{A_c U_L}\left[1 - \exp - \left(\frac{A_c U_L F'}{\dot{m}C_P}\right)\right] \quad (2.6)$$

$$F'' = \frac{F_R}{F'} = \frac{\dot{m}C_P}{A_c U_L F'}\left[1 - \exp - \left(\frac{A_c U_L F'}{\dot{m}C_P}\right)\right] \quad (2.7)$$

The collector flow factor F'' is a function of dimensionless collector capacitance rate, $\frac{\dot{m}C_P}{A_c U_L F'}$. The collector thermal efficiency η_{th} as given by Eq. (2.4) can be written as:

$$\eta_{th} = F_R(\tau\alpha) - \left[F_R U_L \frac{(T_i - T_a)}{I}\right] \quad (2.8)$$

This can be seen to have the form of the equation of straight line, (y = mx + c), as the term F_R and U_L are usually nearly constant over the operating range of the collector. Thus $F_R(\tau\alpha)$ is the intercept and $-F_R U_L$ is the slope of the straight line drawn on a graph with abscissa units of $\left[\frac{(T_i - T_a)}{I}\right]$ and ordinate of η_{th}.

The terms $F_R(\tau\alpha)$ and $F_R U_L$ are used as thermal performance parameters of the flat plate solar collectors.

A solar air heater working on an open cycle which is drawing ambient air outside, the inlet temperature always coincides with the ambient temperature i.e. $T_i = T_a$. Under such operating conditions, the conventional equation (2.4) will not be meaningful as this reduces to $\eta_{th} = F_R(\tau\alpha)$. Therefore, for a solar air heater, it was considered useful

ISSN: 2235-767X
Volume 07 Issue 05
May 2019

to utilize the following equation given by (Duffie and Beckman, 1980; Reddy and Gupta, 1980; Biondi et al., 1988):

$$\eta_{th} = F_0\left[(\tau\alpha) - U_L\frac{(T_o - T_a)}{I}\right] \quad (2.9)$$

where, F_0 is the heat removal factor referred to the outlet temperature expressed as Biondi et al (1988):

$$F_0 = GC_p\left[e^{(U_L F'/GC_p)} - 1\right]\Big/U_L \quad (2.10)$$

Further performance can also be expressed as:

$$\eta_{th} = GC_p\frac{(T_o - T_i)}{I} \quad (2.11)$$

For $T_i = T_a$, the variable reduced temperatures if Eqns. (2.9) and (2.11) coincide. Therefore, Eqns. (2.9) and (2.11) could be represented on a single diagram having the same quantity in the abscissa (Reddy and Gupta, 1980; Biondi et al, 1988). This was considered the most suitable way to describe the characteristic behaviors of solar air collectors (Reddy and Gupta, 1908; Biondi et al, 1988; Khalid et al, 1987).

According to Duffie and Beckman (1980), an approximate analytical correction can be made to $F_R(\tau\alpha)$ and $F_R U_L$ for flow rates for which actual test results are not available. It was proposed that the data be plotted as η_{th} versus $\frac{(T_{av} - T_a)}{I}$ instead of usual $\frac{(T_o - T_i)}{I}$ taking $T_{av} = \frac{T_i + T_o}{2}$. Then the performance equation could be in the form of:

ISSN: 2235-767X
Volume 07 Issue 05
May 2019

$$\eta_{th} = F_{av}(\tau\alpha) - F_{av}U_L\frac{(T_{av}-T_a)}{I} \quad (2.12)$$

where, F_{av} approximated to F' and corrections for $F_R(\tau\alpha)$ and F_RU_L could be obtained from the equations (Duffie and Beckman, 1980) given below:

$$F_R(\tau\alpha) = F_{av}(\tau\alpha)\left[\frac{\dot{m}C_P/A_C}{\dot{m}C_P/A_C + F_{av}U_L/2}\right] \quad (2.13)$$

$$F_RU_L = F_{av}U_L\left[\frac{\dot{m}C_P/A_C}{\dot{m}C_P/A_C + F_{av}U_L/2}\right] \quad (2.14)$$

However, if η_{th} is plotted against $\frac{(T_o-T_a)}{I}$, as is often done for air heater test data (Reddy and Gupta, 1980; Biondi et al, 1988), the equation for η_{th} could be written as:

$$\eta_{th} = F_0(\tau\alpha) - F_0U_L\frac{(T_o-T_a)}{I} \quad (2.15)$$

and then the correction for $F_R(\tau\alpha)$ and F_RU_L would be written as:

$$F_R(\tau\alpha) = F_0(\tau\alpha)\left[\frac{\dot{m}C_P/A_C}{\dot{m}C_P/A_C + F_0U_L}\right] \quad (2.16)$$

$$F_RU_L = F_0U_L\left[\frac{\dot{m}C_P/A_C}{\dot{m}C_P/A_C + F_0U_L}\right] \quad (2.17)$$

ISSN: 2235-767X
Volume 07 Issue 05
May 2019

(Gillet et al. 1983; Bernier and Plett, 1988) declared that the thermal performance representation, testing procedures and mathematical models associated with the solar air collectors had not been developed to the same extent as for liquid collector. The two basic differences between air and liquid collectors are (i) relatively poor thermal conductivity of the air resulting in lower absorber plate to air heat transfer coefficient as compared to that for liquid collectors, which implies that the former have a strong dependence on flow rate, (ii) most air collectors leak since it is not economical to build a perfectly sealed solar air collector.

2.2 PERFORMANCE OF SMOOTH COLLECTOR

An important aspect of the analytical methods of performance prediction of solar air heaters is the heat transfer coefficient in between the absorber plate and air, and the pressure drop in the collector. A number of empirical relations have been predicted for different configurations and working conditions of the collectors. The correlation given by Kays (1966) for heat transfer for flow between parallel plates, with the upper being heated and lower plate insulated has been utilized by Duffie and Beckman (1980) and Khalid et al (1987) for fully developed turbulent flow as:

$$Nu_s = 0.0158\ Re^{0.8} \tag{2.18}$$

For solar air heaters operating in the range of 2000 < Re < 10000, Jansen (1985) utilized the relation recommended by Shewen and Hollands (1980 &1978) based on the data of Kays and London (1964) as:

$$Nu_s = 0.00269\ Re \tag{2.19}$$

The corresponding friction factor was given by Shewen and Hollands (1978) as:

$$f_s = 0.1335\ Re^{-0.317} \tag{2.20}$$

ISSN: 2235-767X
Volume 07 Issue 05
May 2019

The equation suggested by Altemani and Sparrow (1980) for flow in a triangular duct with heated inclined surfaces and an insulated third surface utilized by Khalid et al (1987) for the mass flow rate between 0.01 – 0.05 kg/s.m^2 was given as:

$$Nu_S = 0.019\ Re^{0.781} \tag{2.21}$$

Biondi et al (1988) expressed Kays' Eq. (2.18) by introducing into it, the geometric coefficient of collector given by:

$$K' = \frac{L}{BD^{0.25}} \tag{2.22}$$

$$Nu_S = 0.0158 \left(\frac{GK'}{\mu}\right)^{0.8} D \tag{2.23}$$

For fully developed turbulent flow inside tubes, the correlation for heat transfer and friction factor as recommended by Duffie and Beckman (1980) are:

$$Nu_s = \frac{\left(f_s/8\right) Re\ P_r}{1.07+12.7\sqrt{f_s}\sqrt{8}(p_r^{2/3}-1)} \tag{2.24}$$

$$f_S = [0.79 \ln Re - 1.64]^{-2} \tag{2.25}$$

Prasad and Mullick (1983) recommended for bare cover solar air heater duct in Reynolds number range of 5000 – 25000:

$$Nu_s = 0.014\ p_r^{0.5} f_s^{0.5} Re \tag{2.26}$$

Equation of Malik and Buelow (1975) which agreed within + -10 % for Reynolds number ranging from 10000 – 20000 in solar air heater could be written as:

ISSN: 2235-767X
Volume 07 Issue 05
May 2019

$$Nu_s = \frac{0.01344\ Re^{0.75}}{1-1.586\ Re^{-0.125}} \quad (2.27)$$

The well known equation of Blasius utilized for the calculation of pressure drop for smooth surfaces in solar air heaters (Sukhatme and Nayak, 2008) for 5000 < Re < 30000 is written as:

$$f_s = 0.079Re^{-0.25} \quad (2.28)$$

Another equation in this range (Kays, 1966) is given by:

$$\frac{1}{\sqrt{4f_s}} = -0.8 + 0.87\ln\left(Re\sqrt{4f_s}\right) \quad (2.29)$$

and in the range of 30000 < Re < 100000 Eq. (1.29) closely can be approximated as:

$$f_s = 0.046\ Re^{-0.2} \quad (2.30)$$

Moody chart could also be utilized for friction data in fully developed flow in smooth ducts.

However, a number of researchers have focused their study towards the enhancement of thermal performance of conventional solar air heaters, but are limited to only one side glass cover. As the glass covers provided in solar air heaters affect the thermal performance, the increment in the number of glass covers would be the reason behind the better thermal performance. As such, smooth solar air heaters if provided with glass covers on one absorber plate sides might result in better performance.

2.3 EFFECT OF ROUGHNESS AND FLOW PARAMETERS IN SOLAR AIR HEATERS

European Journal of Business & Social Sciences
Available at https://ejbss.org/
ISSN: 2235-767X
Volume 07 Issue 05
May 2019

Use of artificial roughness of different configurations has been used in plenty to enhance the heat transfer rate in solar air heaters during the last decades. Varying magnitudes of roughness result in varying values of heat transfer and friction factor enhancement. The wide range of relative roughness height covered was 0.001-0.0333. The data was correlated according to the law of wall similarity, by the friction similarity function (Webb et.al., 1971, a,b).

$$u_e^+(e^+) = \sqrt{(2/f)} + 2.5\ln(2e/D) + 3.75 \quad (2.31)$$

Dipprey and Sabersky, (1963) developed a heat momentum transfer analogy relation for flow in sand-grain roughened tubes. One rough tubes were tested, having effective roughness ratios equal to 0.0488, 0.0138 and 0.0024 in the Reynolds number range of 60000 to 500000 in while the Prandtl number ranged from 1.2 to 5.95. The correlation developed was:-

$$\frac{(C_F/2C_H)^{-1}}{\sqrt{(C_F/2)}} + A_f = g(e^+, P_r) \quad (2.32)$$

Based on the approach considered by Han, (1984), analysis for the effect of artificial roughness was made by Prasad and Saini, (1988), for heat transfer and friction factor in a solar air heater using small diameter wire artificial roughness on the top surface, having relative roughness pitch of 10, 15, 20 and relative roughness height of 0.020, 0.027 and 0.033 to predict for a correlation for the average Nusselt number written under as:

$$\overline{Nu} = \frac{\bar{f}/2}{1+\left(\sqrt{\bar{f}/2}\right)\left[4.5(e^+)^{0.28}Pr^{0.57} - 0.95\left(\frac{p}{e}\right)^{0.53}\right]} Re\ Pr \quad (2.33)$$

ISSN: 2235-767X
Volume 07 Issue 05
May 2019

(Han et al., 1991) studied the effect of parallel and V-shaped staggered discrete ribs and found out that 60^0 staggered discrete V-shaped ribs provide higher heat transfer than that for the parallel discrete ribs. Experiments were conducted by (Lau et al., 1991 a, b, c) to study the effect of discrete V-shaped ribs on turbulent heat transfer and friction for fully developed flow of air in a square channel. They found that the average Stanton number for the inclined 45^0 and 60^0 ribs was 20-35% higher than in the 90^0 full rib cases. (Gupta et al, 1993) used transverse wire roughness on the top surface in a solar air heater to investigate for the effect of solar air heater duct aspect ratio and relative roughness height for a relative roughness pitch of 10 and flow Reynolds number of 3000-18000 to arrive at the following correlations:

$$\text{For } e^+ < 35, Nu_r = 0.000824\left(\frac{e}{D}\right)^{-0.178}\left(\frac{W}{H}\right)^{0.288}(Re)^{1.62} \quad (2.34)$$

$$\text{For } e^+ \geq 35, Nu_r = 0.00307\left(\frac{e}{D}\right)^{0.469}\left(\frac{W}{H}\right)^{0.245}(Re)^{0.812} \quad (2.35)$$

Verma and Prasad, (2000) developed the correlation for heat transfer [in a top side artificially roughened solar air heater for fully developed turbulent flow as under:

$$Nu_r = 0.08596\left(\frac{p}{e}\right)^{-0.054}\left(\frac{e}{D}\right)^{0.072}(Re)^{0.728} \quad \text{, for} \quad e^+ \leq 24 \quad (2.36)$$

$$Nu_r = 0.02954\left(\frac{p}{e}\right)^{-0.016}\left(\frac{e}{D}\right)^{0.021}(Re)^{0.802} \quad \text{, for} \quad e^+ > 24 \quad (2.37)$$

(Bhagoria et al., 2002) used wedge shaped transverse repeated rib roughness on one broad heated wall of solar air heater duct and generated data pertinent to friction and heat transfer. They analyzed that the presence of wedge shape ribs yield maximum enhancement in Nusselt number, about 2.4 times as compared to smooth duct. Nusselt number increases and attains maximum value at a wedge angle of about 10^0 and then

ISSN: 2235-767X
Volume 07 Issue 05
May 2019

sharply decreases with increasing wedge angle beyond 10^0. The correlations developed were:-

$$\overline{Nu} = 1.89 \times 10^{-4} Re^{1.21} \left(e/D\right)^{0.426} \left(p/e\right)^{2.94} \times \exp\left[-0.71\left\{\ln\left(p/e\right)\right\}^2\right] \left(\varphi/10\right)^{-0.018} \times \exp\left[-1.5\left\{\ln\left(\varphi/10\right)\right\}^2\right]$$

(2.38)

$$\bar{f} = 12.44\left(e/D\right)^{0.99} \left(\varphi/10\right)^{0.49} Re^{-0.18} \left(p/e\right)^{-0.52} \quad (2.39)$$

(Momin et al., 2002) experimented on flow through duct roughened with V-shape ribs attached to the underside of one broad wall of the duct, to collect data on heat transfer and fluid flow characteristics. They observed that the Nusselt number increases with an increase of Reynolds number. It was found that for relative roughness height of 0.034 and for angle of attack of 60^0, the V-shaped ribs enhance the values of Nusselt number by 1.14 and 2.3 times respectively over inclined ribs and smooth plate case at Reynolds number of 17034 and arrived the correlations as:-

$$\overline{Nu} = 0.067 Re^{0.888} \left(e/D\right)^{0.424} \left(\alpha/60\right)^{-0.077} \times \exp\left[-0.782\left\{\ln\left(\alpha/60\right)\right\}^2\right] \quad (2.40)$$

$$\bar{f} = 6.266\left(e/D\right)^{0.565} \left(\alpha/60\right)^{-0.093} Re^{-0.425} \exp\left[-0.719\ln\left(\alpha/60\right)^2\right] \quad (2.41)$$

Karwa, (2003) had conducted experimental study on heat transfer and friction characteristics in a high aspect ratio duct with transverse, inclined, V-up continuous and V-down continuous, V-up discrete ribs and V-down discrete ribs. He investigated that enhancement in Stanton number over smooth duct was found to be 65-90%, 87-112%, 102-137%, 110-147%, 93-134% and 102-142% respectively. The friction factor ratio for V-up continuous and V-down continuous, V-up discrete ribs and V-down discrete ribs was found to be 3.92, 3.65, 2.47 and 2.58 respectively and the correlations arrived are:

ISSN: 2235-767X
Volume 07 Issue 05
May 2019

$$G = 32.26e^{-0.006}(W/H)^{0.5}(p/e)^{2.56}\exp[0.7343\{\ln(p/e)\}^2](e^+)^{-0.08} \quad (2.42)$$

For $7 \leq e^+ \leq 20$

$$R = 1.66(e^+)^{-0.0078}(W/H)^{-0.4}(p/e)^{2.695}\exp[-0.762\{\ln(p/e)\}^2(e^+)^{-0.075}] \quad (2.43)$$

For $20 \leq e^+ \leq 60$

$$R = 1.325(e^+)^{-0.0078}(W/H)^{-0.4}(p/e)^{2.695}\exp[-0.762\{\ln(p/e)\}^2] \quad (2.44)$$

(Cho et al., 2003) experimentally investigated the effect of gap in the inclined ribs on heat transfer in square duct with rib to pitch height ratio of 8 and angle of attack of 60^0.Experiments were carried out by maintaining the gap width same as the rib width and by varying the gap position over the duct width for parallel and cross rib arrangement on two opposite walls, they investigated that, the inclined rib with a downstream gap shows significant enhancement in heat transfer as compared to that of continuous inclined rib arrangement.

The effect of relative roughness pitch, relative roughness height and relative groove position on the heat transfer coefficient and friction factor has been studied experimentally by (Jaurkur et al., 2006) using rib-grooved roughness and the correlations arrived are:

$$Nu = 0.00206Re^{0.936}(e/D)^{0.349}(p/e)^{3.318}\exp[-0.868\{\ln(p/e)\}^2](g/p)^{1.108}\exp[2.486\{\ln(g/p)\}^2 + 1.405\{\ln(g/p)\}^3] \quad (2.45)$$

$$f = 0.0012Re^{-0.199}(e/D)^{0.585}(p/e)^{7.19}\exp[-1.854\{\ln(p/e)\}^2](g/p)^{0.645}\exp[1.513\{\ln(g/p)\}^2 + 0.8662\{\ln(g/p)\}^3] \quad (2.46)$$

ISSN: 2235-767X
Volume 07 Issue 05
May 2019

CFD investigation using ten different ribs namely rectangular, square, chamfered, triangular etc. is done by (Chaube et al., 2006). FLUENT CFD code is used for analysis using the SST k-ε turbulence model. The heat flux of 1100 W/m^2 is provided on the absorber plate only and rib surface is kept adiabatic. Their study reported that highest heat transfer is achieved with chamfered ribs and the best performance index is found with rectangular ribs of size 3×5.

(Karmare et al., 2007) experimentally study the effect of heat transfer performance of a rectangular duct with metal grit ribs as roughness element, employed on one broad wall, transferring heat to the air flowing through it. The effect of relative length, height and pitch of the metal grid ribs on the heat transfer and friction factor has been studied for the flow range of Reynolds numbers 4000-17000. It has been found that maximum heat transfer rate was reported for the set of parameters and maximum friction factor was observed for the set of parameters. Correlations for Nusselt number and friction factor were developed based on the experimental results and were given by:

$$Nu = 2.4Re^{1/3}(e/D)^{0.42}(l/s)^{-0.146}(p/e)^{-0.27} \quad (2.47)$$

$$f = 15.55Re^{-0.26}(e/D)^{0.94}(l/s)^{-0.27}(p/e)^{-0.51} \quad (2.48)$$

(Varun et al., 2008) experimentally used a combination of transverse and inclined ribs as roughness geometry and examined the thermal performance for the range of Reynolds number (Re), 2000-14000, pitch of ribs (p), 5-13 mm, roughness height (e), 1.6 mm and aspect ratio (W/H), of 10. Results show that the collector roughened with this type of roughness provides best performance at relative roughness pitch (p/e) of 8 and the correlations developed were:-

$$\bar{f} = 1.0858(Re)^{-0.3685}(p/e)^{0.0114} \quad (2.49)$$

ISSN: 2235-767X
Volume 07 Issue 05
May 2019

$$\overline{Nu} = 0.0006(Re)^{1.213}(^{p}/_{e})^{0.0104} \quad (2.50)$$

(Ahrwal et al., 2008) studied the effect of width and position of gap in inclined split-ribs having square cross section on heat transfer and friction characteristics of a rectangular air heater duct. The increase in Nusselt number and friction factor was in the range of 1.48-2.59 times and 2.26-2.9 times of the smooth duct respectively for the range of Reynolds numbers from 3000-18000 and the correlations arrived are:

$$Nu = 0.0102Re^{1.148}(e/D)^{0.51}[1 - \{0.25 - d/w^2(0.01(1 - g/e)^2)\}] \quad (2.51)$$

$$f = 0.5Re^{-0.0836}(e/D)^{0.72} \quad (2.52)$$

Karwa and Maheshwari, (2009) made an experimental study of heat transfer and friction in a rectangular section duct with fully perforated baffles or half perforated baffles at relative roughness pitch of 7.2-28.8 affixed to one of the broader walls. They investigated that there was enhancement of 79-169% in Nusselt number over the smooth duct for the fully perforated baffles and 133-274% for the half perforated baffles while the friction factor for fully perforated baffles was found to be 2.98-8.02 times of that for the smooth duct and 4.42-17.5 times for the half perforated baffles. The correlations arrived are:

$$Nu = 0.0893\ Re^{0.7608} \quad (2.53)$$

$$f = 0.1673\ Re^{-0.0213} \quad (2.54)$$

An experimental investigation had been carried out by Bopche and Tandale, (2009) to study the heat transfer coefficient and friction factor by using artificially roughness in the form of inverted U-shaped turbulators, on the absorber surface of an air heater duct. As compared to smooth one, the enhancement in heat transfer and friction factor was reported of the order of 2.82 and 3.72 times, respectively and the correlations developed are:

$$Nu = 0.5429Re^{0.7054}(e/D)^{0.3619}(p/e)^{-0.1592} \quad (2.55)$$

$$f = 1.2134Re^{-0.2076}(e/D)^{0.3285}(p/e)^{-0.4259} \quad (2.56)$$

ISSN: 2235-767X
Volume 07 Issue 05
May 2019

Sriromrein and Promvong, (2010) studied that heat transfer and friction characteristic of a rectangular duct roughened artificially with Z-shaped ribs. The enhancement in heat transfer rate and best thermal performance was reported for Z-rib inclined at 45^0. (Hans et al., 2010) developed multiple V-rib roughness and performed extensive experimentation to collect data on heat transfer and fluid flow characteristics of a roughened duct. Maximum enhancement in Nusselt number and friction factor due to presence of multi v-rib roughness has been found to be 6 and 5 times, respectively, in comparison to the smooth duct. The maximum enhancement in heat transfer has been achieved corresponding to relative roughness width (W/w) of 6. It has been observed that Nusselt number attain maximum value at 60^0angle of attack. The correlations proposed were:-

$$\overline{Nu} = 3.35 \times 10^{-5} Re^{0.92} \left(e/D\right)^{0.77} \left(W/w\right)^{0.43} \left(\alpha/90\right)^{-0.49} \times \exp^{\left[-0.1177\{\ln(W/w)\}^2\right]} \times \exp^{\left[-0.61\{\ln(\alpha/90)\}^2\right]} \left(p/e\right)^{8.54} \times \exp^{\left[-2.0407\{\ln(p/e)\}^2\right]}$$

(2.57)

$$\bar{f} = 4.47 \times 10^{-4} Re^{-0.3188} \left(e/D\right)^{0.73} \left(W/w\right)^{0.22} \left(\alpha/90\right)^{-0.39} \times \exp\left[-0.52\left(\ln\left(\frac{\alpha}{90}\right)\right)^2\right] \left(p/e\right)^{8.9} \exp\left[-2.133\left(\ln\left(p/e\right)\right)^2\right]$$

(2.58)

However, in all the above cases, provision of artificial roughness and glass cover has remained limited to only one side (top side) of the solar air heater duct except those of the recent ones (Prasad et al., 2014 and Behura et al., 2016), wherein it has been concluded that one sides roughened and glass covered solar air heaters perform even better than those of one side roughened and glass covered solar air heaters, but friction factor also increases.

European Journal of Business & Social Sciences
Available at https://ejbss.org/
ISSN: 2235-767X
Volume 07 Issue 05
May 2019

CHAPTER 3

EXPERIMENTAL SET-UP

Although there are a number of analytical and experimental works have been investigated on heat transfer and fluid flow characteristics in artificially roughened ducts, as available in the literature, but there are very few experimental data to verify the expressions, that have been developed (Prasad et al., 2014) and investigated (Behura et al., 2016), only for rectangular solar air heater ducts with one sides roughness and glass covers. Apart from the requirement of experimental verification of solar air heaters with artificially roughened absorber plate also needs to be optimized and investigated in order to produce design data for such systems.

In view of this, a novel experimentation work has been planned to produce heat transfer, fluid flow and thermal & thermo hydraulic performance data for the optimal condition on solar air heaters using absorber plate with one sides artificial roughness and glass covers simultaneously with the one sides glass covered roughness with booster mirror ones. This chapter has been devoted to explain solar air heater ducts, instrumentation, the experimental set-up and the procedure of experimentation.

Figs.3.1 Shows the top view of experimental set-up respectively, combining the two In both the roughened and glass covered solar air heater ducts, the roughness elements have been provided on the flow side of the absorber plate normal to the ambient air flow direction at varying values of relative roughness pitch, p/e equal to 16, relative roughness height, e/D equal to 0.048, flow Reynolds number, Re, in the range of 2000-7000 and mass flow rate, $\dot{m}$, solar air heater ducts with a single blower to run simultaneously. Directions denoted by arrows X and Y represent the ambient air flow in both the roughened ducts. Both the ducts are having one side glass covers.

European Journal of Business & Social Sciences
Available at https://ejbss.org/
ISSN: 2235-767X
Volume 07 Issue 05
May 2019

Thermocouples were provided on the collectors to measure temperature distribution, while digital thermometers were used to measure the temperature distribution in the air duct. The output of thermocouple fed to digital voltmeter displays directly the temperature values. Mass flow rate was varied by controlling the blower speed by means of a single phase auto variac. Mass flow rate for a particular run for both the solar air heaters was measured by means of two separate flange tape orifice-meters, provided with U-tube manometers.

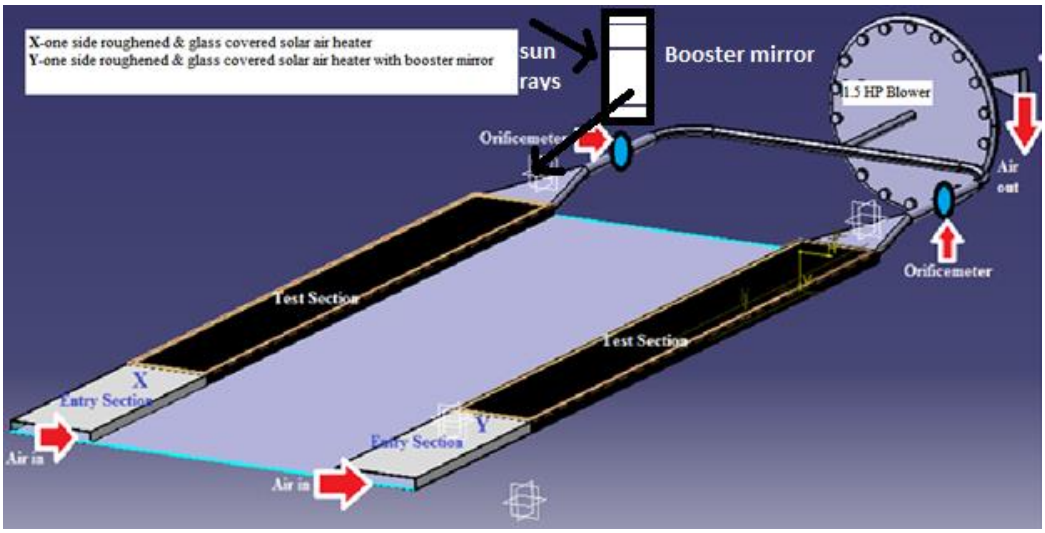

Fig. 3.1 Top view of the experimental set-up

European Journal of Business & Social Sciences
Available at https://ejbss.org/
ISSN: 2235-767X
Volume 07 Issue 05
May 2019

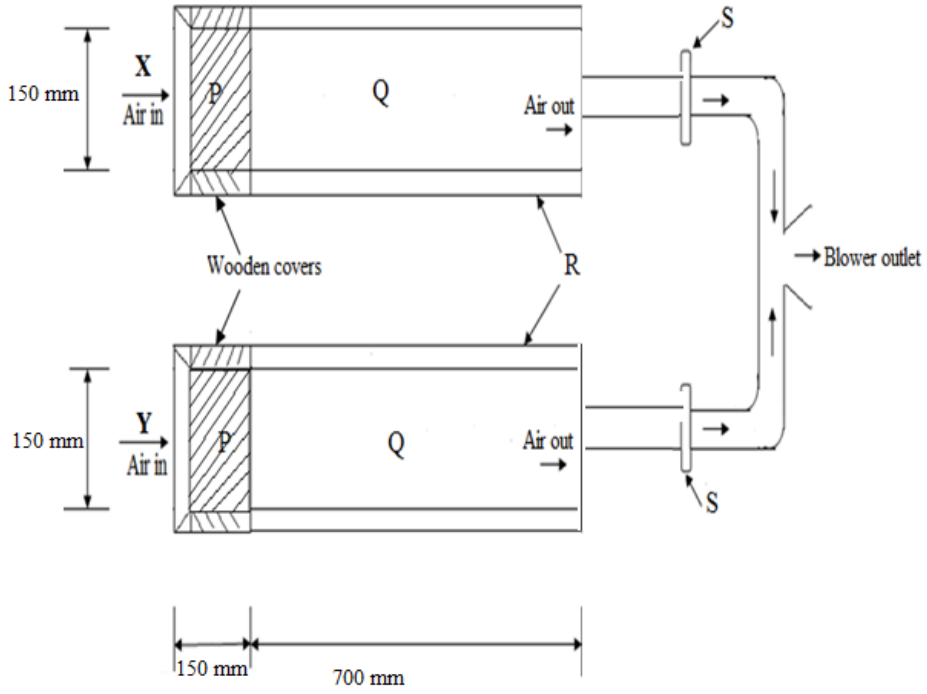

All dimensions are in mm

X-One sides roughened and glass covered solar air heater

Y-One sides roughened and glass covered solar air heater with booster mirror

P-Unheated wooden covered entry section

Q-Glass covered test section

R-Glass covers

S-Flange tape orifice-meters

Fig. 3.2 Schematic diagram of the experimental set-up

European Journal of Business & Social Sciences
Available at https://ejbss.org/
ISSN: 2235-767X
Volume 07 Issue 05
May 2019

3.1SOLAR AIR HEATER DUCTS

Figs.3.3 (a) & (b) shows the two solar air heater duct models of similar size having high **1** aspect ratio: (1) roughened with one sides glass covers and (2) one sides roughened with booster mirror.Circular wire of different diameters has been provided on the absorber plate at varying pitches to serve as an artificial roughness element. The two ducts have been made similar in all dimensions to achieve direct comparison between the fluid flow as well as the heat transfer characteristics of the two ducts in order to determine the enhancement of thermal and thermo hydraulic performance parameters under similar conditions. Ambient air has been sucked by two separate inlets but, exhausted by means of a single outlet. A common bottom sheet of 850 mm × 150 mm wooden piece with 25 mm thickness has been used for insulation. The two separate one sides glass covers (700 mm × 150 mm) have been provided. An air gap of 25 mm has been provided in between the bottom and absorber plate for each duct resulted in a duct cross section of 150 mm × 80 mm each.

European Journal of Business & Social Sciences
Available at https://ejbss.org/
ISSN: 2235-767X
Volume 07 Issue 05
May 2019

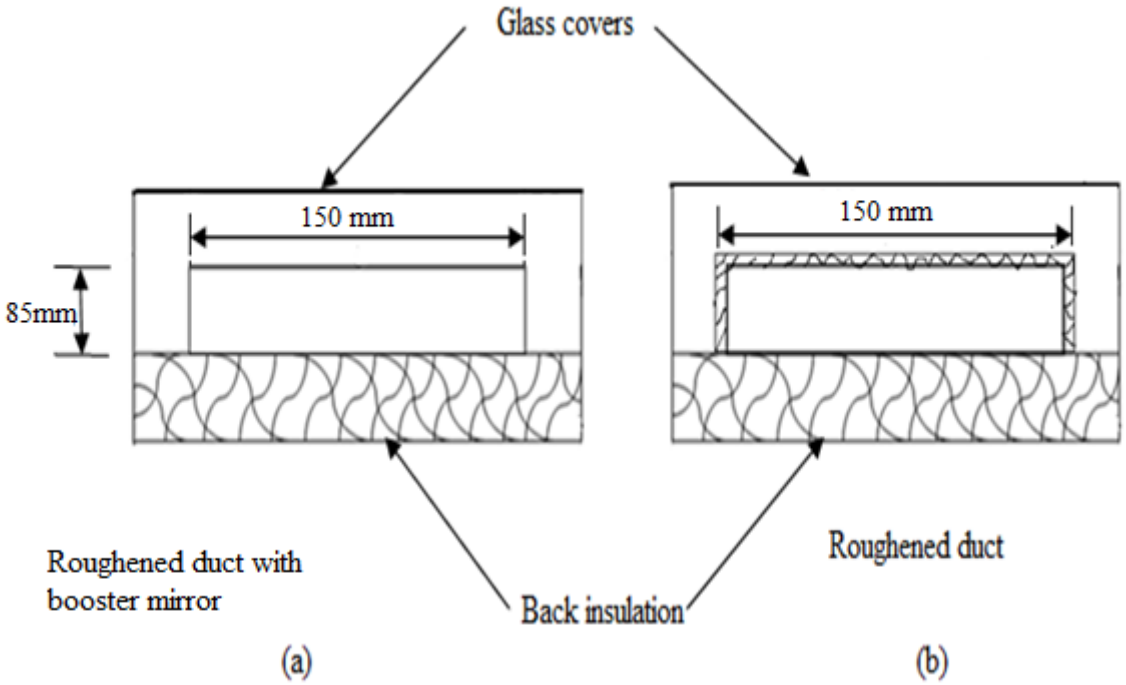

Figs. 3.3 (a) and (b) Solar air heater duct models

Out of the total duct length of 850 mm, the last 700 mm portion was utilized for instrumentation and the balance length of 150 mm was served as the entry length for flow stabilization. in the range of $8.35 \times 10^{-3} - 3.75 \times 10^{-2}$.

European Journal of Business & Social Sciences
Available at https://ejbss.org/
ISSN: 2235-767X
Volume 07 Issue 05
May 2019

CHAPTER 4

EXPERIMENTAL PROCEDURE

4.1 Experimental Procedure

Test runs were conducted under controlled conditions of mass flow rate (i.e. flow Reynolds number, Re) and the roughness parameters $(p/e, e/D)$, under actual outdoor conditions with varying values of solar radiation intensity and ambient temperature. Test data were collected at quarter hourly intervals each day between 11 AM and 2 PM in the months of April 2018. Parameters measured were:

- Pressure difference across orifice-meter
- Pressure drop across inclined tube manometer
- Temperature of the absorber plates
- Temperature of air flowing in the duct
- Ambient temperature

In 7 numbers of runs, 1 set of one side roughened absorber plate, along with the 1 set of one side roughened absorber plate with booster mirror at varying mass flow rates were tested (Table- 4.1).

Set No.	Run no.	Date	$\dot{m}$,(Kg/s)	Re	P,(mm)	e,(mm)	p/e	e/D

European Journal of Business & Social Sciences
Available at https://ejbss.org/
ISSN: 2235-767X
Volume 07 Issue 05
May 2019

1	1	20.04.2018	0.0375	7013	15.0	0.9	16	0.042
	2	23.04.2018	0.0282	6772				
	3	24.04.2018	0.0271	6127				
	4	25.04.2018	0.0187	5749				
	5	26.04.2018	0.0175	4894				
	6	27.04.2018	0.0118	3166				
	7	30.04.2018	0.0085	2356				
2	8	01.05.2018	0.0361	6693	14.4	0.8	18	0.051
	9	02.05.2018	0.0274	6662				
	10	03.05.2018	0.0261	6115				
	11	04.05.2018	0.0167	5701				
	12	07.05.2018	0.0155	4714				
	13	08.05.2018	0.0012	3231				
	14	11.05.2018	0.0075	2302				

Table- 4.1 Range of parameters investigated

European Journal of Business & Social Sciences
Available at https://ejbss.org/
ISSN: 2235-767X
Volume 07 Issue 05
May 2019

CHAPTER – 5

RESULTS AND DISCUSSIONS

5.1 INTRODUCTION

As discussed earlier, provision of artificial roughness and glass covers is one of the vital reason for the enhancement of thermal and thermo hydraulic performance off solar air heaters. The present chapter reports the data presentation, reduction and its validation. Based on the experimental results, correlations of Nusselt number and friction factor have been developed as a function of flow and roughness parameters. The effect of roughness and flow parameters on heat transfer, friction factor have been shown.

5.2 EXPERIMENTAL DATA

The raw experimental data during experimentation for Run no. 6, which included thermocouple readings, ambient temperatures, and temperature of air in the ducts, mass flow rates, pressure drop in ducts, have been tabulated in Table – 4.1.

5.2.1 Observation tables for set 1

European Journal of Business & Social Sciences
Available at https://ejbss.org/
ISSN: 2235-767X
Volume 07 Issue 05
May 2019

Date: 20/04/2019

Time	Box	Ta1	Ta2	Ta3	Tp1	Tp2	Tp3
11:00	R	32	32	33	50	49	48
	RB	36	37	37	59	58	58
11:30	R	33	33	34	49	48	48
	RB	37	38	38	59	58	57
12:00	R	33	34	34	48	47	47
	RB	38	38	39	58	57	56
12:30	R	34	35	35	47	47	46
	RB	39	39	40	57	57	55
1:00	R	35	36	36	46	46	45
	RB	30	40	40	56	55	54
1:30	R	36	37	38	46	45	44
	RB	40	41	41	56	54	54
2:00	R	37	38	38	45	44	44
	RB	41	41	42	55	54	53
2:30	R	38	39	40	44	44	43
	RB	42	42	43	55	53	53
3:00	R	40	40	41	43	42	41
	RB	42	43	44	54	53	52

European Journal of Business & Social Sciences
Available at https://ejbss.org/
ISSN: 2235-767X
Volume 07 Issue 05
May 2019

Table-5.1 Test data collected during a typical run (Run no. 1)

Date: 23/04/2019

Time	Box	Ta1	Ta2	Ta3	Tp1	Tp2	Tp3
11:00	R	30	30	31	49	48	47
	RB	36	37	37	58	57	57
11:30	R	30	31	31	48	48	47
	RB	37	37	38	58	57	56
12:00	R	31	31	32	47	47	46
	RB	37	38	39	57	56	56
12:30	R	31	32	33	47	46	45
	RB	39	39	40	56	55	55
1:00	R	32	32	34	46	45	45
	RB	39	40	40	55	55	54
1:30	R	33	32	35	45	45	44
	RB	39	40	41	55	54	54
2:00	R	34	34	35	44	44	43
	RB	40	41	42	55	54	53
2:30	R	34	35	36	44	43	42
	RB	41	42	42	53	53	52
3:00	R	35	36	37	42	42	41
	RB	42	43	44	52	52	51

European Journal of Business & Social Sciences
Available at https://ejbss.org/
ISSN: 2235-767X
Volume 07 Issue 05
May 2019

Table-5.2 Test data collected during a typical run (Run no. 2)

Date: 24/04/2019

Time	Box	Ta1	Ta2	Ta3	Tp1	Tp2	Tp3
11:00	R	33	33	33	49	49	48
	RB	35	35	36	57	57	56
11:30	R	33	34	34	49	48	48
	RB	35	36	36	57	56	56
12:00	R	33	34	35	48	48	47
	RB	36	37	38	56	56	55
12:30	R	34	35	36	48	47	47
	RB	37	38	38	56	55	54
1:00	R	34	36	36	48	47	46
	RB	38	38	39	56	54	54
1:30	R	35	36	37	47	47	46
	RB	39	40	41	55	54	53
2:00	R	36	37	37	46	46	45
	RB	40	41	42	55	54	52
2:30	R	37	37	38	46	45	44
	RB	41	41	42	54	53	52
3:00	R	38	39	40	45	44	43

European Journal of Business & Social Sciences
Available at https://ejbss.org/
ISSN: 2235-767X
Volume 07 Issue 05
May 2019

	RB	41	42	43	53	52	51

Table-5.3 Test data collected during a typical run (Run no. 3)

Date: 25/04/2019

Time	Box	Ta1	Ta2	Ta3	Tp1	Tp2	Tp3
11:00	R	32	32	33	50	50	50
	RB	37	37	38	58	58	57
11:30	R	32	33	33	50	50	49
	RB	37	38	38	57	56	55
12:00	R	33	34	35	49	49	48
	RB	37	38	39	57	56	55
12:30	R	33	34	36	49	48	47
	RB	38	38	39	57	55	54
1:00	R	34	35	36	48	48	46
	RB	38	39	40	56	55	53
1:30	R	35	36	36	48	47	46
	RB	39	40	40	55	54	53
2:00	R	36	36	37	47	47	46
	RB	40	41	42	55	53	52
2:30	R	37	37	38	47	46	45
	RB	41	42	43	54	53	52

ISSN: 2235-767X
Volume 07 Issue 05
May 2019

3:00	R	37	38	39	46	45	44
	RB	42	43	44	53	52	51

Table-5.4 Test data collected during a typical run (Run no. 4)

Date: 26/04/2019

Time	Box	Ta1	Ta2	Ta3	Tp1	Tp2	Tp3
11:00	R	31	31	32	48	48	47
	RB	36	37	37	56	55	55
11:30	R	31	32	33	48	47	47
	RB	36	37	38	55	54	54
12:00	R	32	33	33	47	46	46
	RB	37	38	39	55	54	53
12:30	R	33	34	34	47	46	45
	RB	37	39	39	54	54	53
1:00	R	33	34	35	46	46	45
	RB	38	39	40	54	53	52
1:30	R	34	34	35	46	45	44
	RB	39	39	40	53	52	51
2:00	R	34	35	36	45	44	44
	RB	39	40	41	53	51	51
2:30	R	35	36	37	45	44	43

ISSN: 2235-767X
Volume 07 Issue 05
May 2019

	RB	40	40	41	52	51	50
3:00	R	36	36	38	44	43	42
	RB	40	41	42	51	50	49

Table-5.5 Test data collected during a typical run (Run no. 5)

Date: 27/04/2019

Time	Box	Ta1	Ta2	Ta3	Tp1	Tp2	Tp3
11:00	R	32	32	33	49	49	48
	RB	37	37	38	56	55	55
11:30	R	33	34	35	49	48	48
	RB	37	38	39	56	55	54
12:00	R	34	34	35	48	48	47
	RB	38	38	39	55	54	53
12:30	R	34	35	36	48	47	46
	RB	38	39	40	54	53	53
1:00	R	35	35	36	47	46	45
	RB	39	39	40	54	53	52
1:30	R	36	36	37	46	46	45
	RB	39	40	41	53	52	51
2:00	R	36	37	38	46	45	44
	RB	40	41	42	52	52	51

ISSN: 2235-767X
Volume 07 Issue 05
May 2019

2:30	R	37	37	38	46	44	44
	RB	41	42	42	52	51	50
3:00	R	37	38	39	45	44	43
	RB	41	42	43	51	50	49

Table-5.6 Test data collected during a typical run (Run no. 6)

Date: 30/04/2019

Time	Box	Ta1	Ta2	Ta3	Tp1	Tp2	Tp3
11:00	R	31	31	32	49	48	48
	RB	35	35	36	58	57	56
11:30	R	31	32	32	48	48	47
	RB	35	36	37	56	55	55
12:00	R	32	32	33	47	46	46
	RB	36	36	37	55	54	54
12:30	R	32	33	34	46	45	44
	RB	36	37	38	54	54	53
1:00	R	33	34	35	45	44	44
	RB	37	37	38	54	53	53
1:30	R	34	34	35	44	43	43
	RB	37	38	38	53	53	52
2:00	R	34	35	36	43	43	42

ISSN: 2235-767X
Volume 07 Issue 05
May 2019

	RB	38	38	39	53	52	52
2:30	R	35	35	36	42	42	41
	RB	39	40	40	52	51	51
3:00	R	36	37	38	41	41	40
	RB	39	40	41	51	51	50

Table-5.7 Test data collected during a typical run (Run no. 7)

5.3 Sample Results

Typical values for different parameters have been listed in Table- 5.6 for Run no.6.

Time (hours)	T_a, ^{0}C	$\bar{S}_{trb}$	S_{tr}	h_{rb}, W/m^{2}K	$\overline{Nu}_{rb}$	h_r, W/m^{2}K	Nu_r
11.00	29.0	0.02286	0.01337	46.73	78.18	26.37	45.73
11.15	29.2	0.02287	0.01341	47.84	78.23	27.48	45.84
11.30	29.6	0.02257	0.01308	46.72	77.18	26.27	44.72
11.45	30.4	0.02288	0.01339	47.73	78.27	27.94	45.81
12.00	30.9	0.02259	0.01292	46.62	77.27	26.27	44.17
12.15	31.3	0.02253	0.01289	46.09	77.06	26.91	44.06
12.30	31.8	0.02283	0.01319	47.13	78.09	27.31	45.11
12.45	32.3	0.02284	0.01318	47.12	78.11	27.21	45.09
13.00	33.1	0.02289	0.01327	47.39	78.29	27.93	45.37
13.15	33.5	0.02262	0.01295	46.29	77.37	26.92	44.29

ISSN: 2235-767X
Volume 07 Issue 05
May 2019

13.30	34.1	0.02299	0.01317	47.02	78.02	27.21	45.02
13.45	34.7	0.02274	0.01311	46.81	77.79	26.18	44.81
14.00	35.1	0.02304	0.01340	47.78	78.81	27.87	45.79

Table- 5.8 Values of T_a, h, S_t and Nu as a function of time during the day (Run no. 6)

5.4 VALIDATION OF THE EXPERIMENTAL DATA

The values of Nu and f obtained from experimental data for smooth solar air heater have been compared to the values obtained from Dittus-Boelter equation for Nu and modified Blasius equation for f,which are reproduced below, written under as the following Eqs.(5.11) and (5.12):

$Nu = 0.023Re^{0.8}P_r^{0.4}$ (Dittus-Boelter equation) (5.11)

$f = 0.085Re^{-0.25}$ (Modified Blasius equation) (5.12)

European Journal of Business & Social Sciences
Available at https://ejbss.org/
ISSN: 2235-767X
Volume 07 Issue 05
May 2019

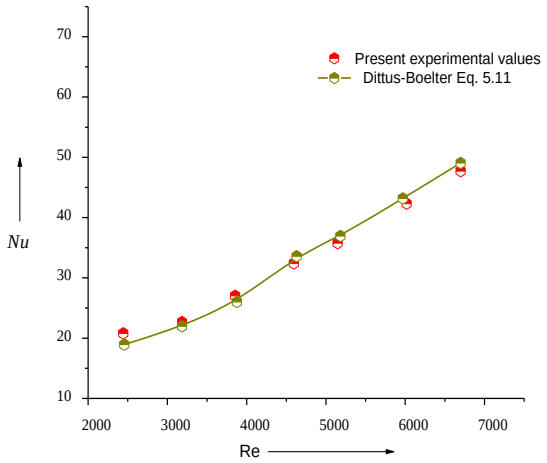

Fig. 5.1 Validity curve for experimental values of Nusselt number

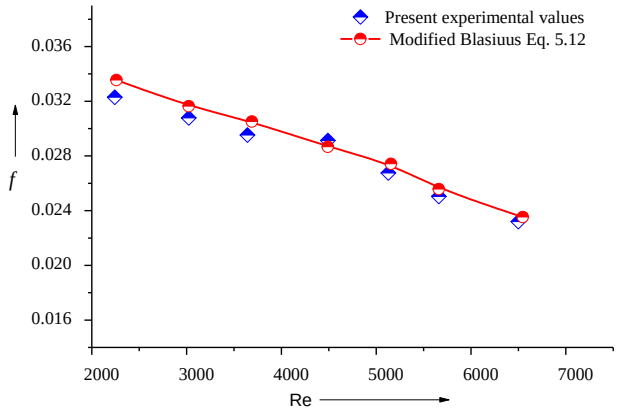

Fig. 5.2 Validity curve for experimental values of friction factor

Comparison of the referred and present experimental values of Nusselt number and friction factor has been shown in Figs. 5.1 and 5.2, respectively. The average deviations

ISSN: 2235-767X
Volume 07 Issue 05
May 2019

between experimental values of Nu &f, and the values predicted by Eqs. (5.11) and (5.12), have been found to be $\pm$2.7 and $\pm$2.5, respectively, that shows a good agreement between the two sets of values, ensuring the accuracy of the present data collected with the experimental set-up.

5.5 EFFECT OF ROUGHNESS AND FLOW PARAMETERS

5.5.1 Effect of p/e and e/D on Stanton number

Figs. 5.3 shows the effect of the roughness and flow parameters p/e, e/D and Re on Stanton number in one sides roughened and roughened with booster mirror one. It could be seen from these figures that the values of Stanton number in one sides roughened collector with and without booster mirrors decrease with increasing values of relative roughness pitch, p/e, for a given value of relative roughness height, e/D and decreasing values of relative roughness height, e/D, for a given value of relative roughness pitch, p/e. The values of Stanton number are found to decrease with increasing values of flow Reynolds number. It could be worked out from Figs. 5.3 that the values of Stanton number are more in one sides roughened with booster one in the range of 36% to 48%, as compared to without booster mirror ones.

5.5.2 Effect of p/e and e/D on friction factor

Fig. 5.4 shows the effect of p/e on friction factor for a given value of e/D. It could be seen from the figure that the values of friction factor increase with decrease in the value of the relative roughness pitch,p/e, and decrease with increasing values of the flow Reynolds number, Re. The values of friction factor in are more in one sides roughened with booster one in the range of 28% to 38%, as compared to without booster mirror ones**.**

5.5.3 Effect of p/e and e/D on Nusselt number

European Journal of Business & Social Sciences
Available at https://ejbss.org/
ISSN: 2235-767X
Volume 07 Issue 05
May 2019

Fig. 5.5 shows the effect of p/e on friction factor for a given value of e/D. It could be seen from the figure that the values of Nusselt number increase with increase in the value of the relative roughness pitch,p/e, and increase with increasing values of the flow Reynolds number, Re. The values of Nusselt number in are more in one sides roughened with booster one in the range of 31% to 43%, as compared to without booster mirror ones**.**

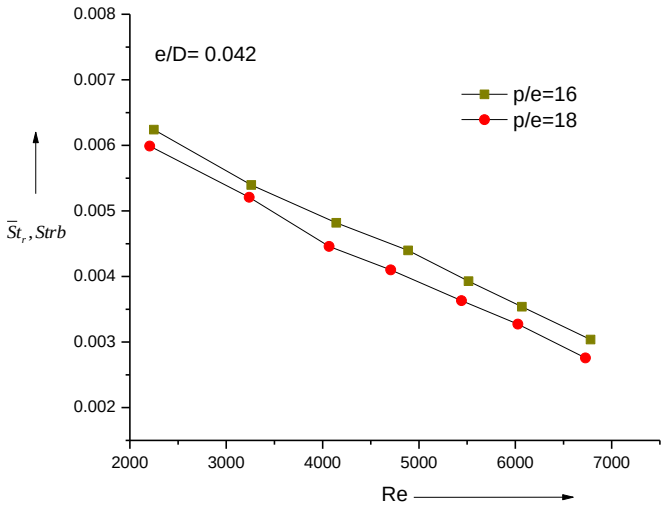

Fig.5.3 Effect of p/e on Stanton number in one sides artificially roughened solar air heater with and without booster mirror

European Journal of Business & Social Sciences
Available at https://ejbss.org/
ISSN: 2235-767X
Volume 07 Issue 05
May 2019

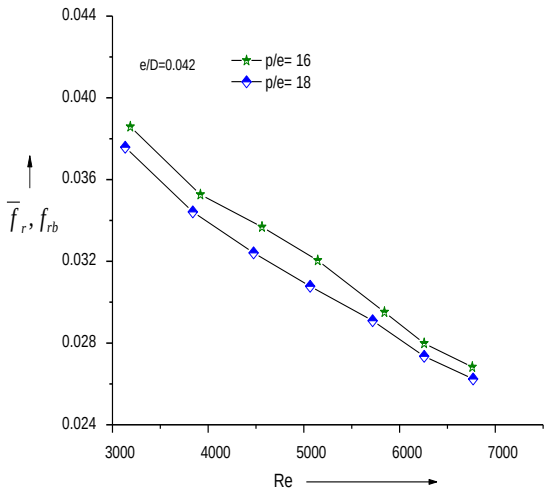

Fig. 5.4 Effect of p/e on friction factor in one sides artificially roughened solar air heater with and without booster mirror

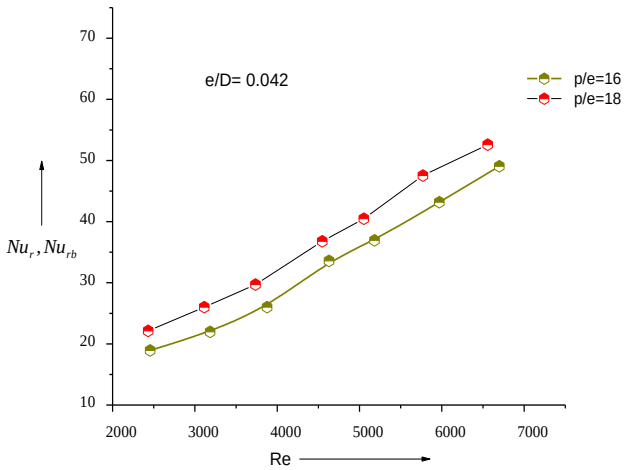

European Journal of Business & Social Sciences
Available at https://ejbss.org/
ISSN: 2235-767X
Volume 07 Issue 05
May 2019

Fig. 5.5 Effect of p/e on Nusselt number in one sides artificially roughened solar air heater with and without booster mirror

5.6 THERMAL PERFORMANCE

Fig. 5.6 represents typically the performance characteristics of the roughened solar air heaters for p/e =16, e/D = 0.042: (i) one side roughened and glass covered, (ii) top side roughened and glass covered with booster mirror arrangement, all at varying mass flow rates.

The efficiency data values worked out by the following instantaneous thermal performance Eq. (5.13):

$$\eta_{th} = \dot{m}C_p(T_0 - T_i)/IA_C \quad (5.13)$$

shown by the respective lines are represented for each mass flow rate from the origin, resulting in the respective lines for the respective mass flow rates. Utilizing the efficiency data values, the respective curves A$-B_{1rb}$ and $C - D_{1r}$, have been obtained by the least square fit method for both the cases. As could be seen from this figure that top side roughened and glass covered solar air heater with booster mirror has higher value of thermal efficiency than those of only one side roughened and glass covered solar air heater.

European Journal of Business & Social Sciences
Available at https://ejbss.org/
ISSN: 2235-767X
Volume 07 Issue 05
May 2019

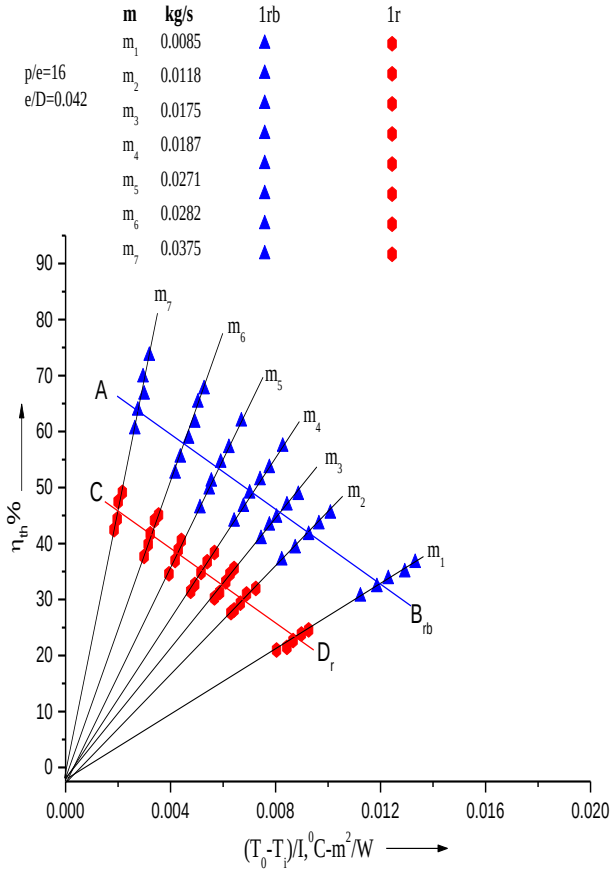

Fig 5.6 Performance characteristics of solar air heaters

It could be attributed that the top side roughened and glass covered solar air heater with the provision of booster mirror is 40 to 47% more efficient than that of without booster mirror one.

European Journal of Business & Social Sciences
Available at https://ejbss.org/
ISSN: 2235-767X
Volume 07 Issue 05
May 2019

CHAPTER 6

CONCLUSIONS

On the basis of present work the following conclusions have been drawn:-

1. The values of Stanton number are more in one sides roughened with booster one in the range of 36% to 48%, as compared to without booster mirror ones.
2. The values of friction factor in are more in one sides roughened with booster one in the range of 28% to 38%, as compared to without booster mirror ones**.**
3. The values of Nusselt number in are more in one sides roughened with booster one in the range of 31% to 43%, as compared to without booster mirror ones**.**
4. The top side roughened and glass covered solar air heater with the provision of booster mirror is 40 to 47% more efficient than that of without booster mirror one.

European Journal of Business & Social Sciences
Available at https://ejbss.org/
ISSN: 2235-767X
Volume 07 Issue 05
May 2019

CHAPTER 7

FUTURE SCOPE

The present work has been investigated for the optimal thermo hydraulic performance of one sides roughened and glass covered solar air heaters by providing transverse wire roughness. The work may be extended to:

1. Use of one sides inclined wire roughness in such solar air heaters may enhance the heat transfer rate and hence may give better thermal and thermo hydraulic performance.
2. Use of booster mirror in such solar air heaters with three sides artificially roughened one may be the reason behind better performance.

ISSN: 2235-767X
Volume 07 Issue 05
May 2019

REFRENCES

Aharwal, K. R., Gandhi, B. k. and Saini, J. S., 2008. Experimental investigation on heat transfer enhancement due to a gap in an inclined continuous rib arrangement in a rectangular duct of solar air heater, Renew. Energy, 33, 585-596.

Altermani, C.A.C. and Sparow, E.M., 1980. Turbulent heat transfer and fluid flow in an unsymmetrically heated triangular duct, Trans. ASME, J. Heat Mass Transfer, 102, 590.

Behura, K.Arun**,** Prasad, B. N., Prasad, L., 2016. Heat transfer, friction factor and thermal performance of one sides artificially roughened solar air heaters. Sol. Energy. 130, 46-59.

Bernier, M.A. and Plett, E.G., 1988. Thermal performance representation and testing of air solar collectors, Trans. ASME, 110, 74-81.

Bhagoria, J. L., Saini, J. S. and Solanki, S. C., 2002. Heat transfer coefficient and friction factor correlations for rectangular solar air heater duct having transverse wedge shaped rib roughness on the absorber plate, Renew. Energy, 25, 341-369.

ISSN: 2235-767X
Volume 07 Issue 05
May 2019

Bhushan, B. and Singh, R., 2011. Nusselt number and friction factor correlations for solar air heater duct having artificially roughened absorber plate, Sol. Energy, 133, 1277-1287.

Biondi, P., Cicala, L. and Farina, G., 1988. Performance analysis of solar air heaters of conventional design, Sol. Energy, 41 (1), 101-107.

Bliss, R.W., 1959. The derivation of several plate efficiency factors useful in the design of flat plate solar heat collectors, Sol. Energy, 3, 55-64.

Bopche, S. B. and Tandale, M. S., 2009. Experimental investigation on heat transfer and frictional characteristics of turbulator roughened solar air heater duct, Int. J. Heat Mass Transfer, 52, 2834-2848.

Chaube, A., Sahoo, P. K. and Solanki, S. C., 2006. Analysis of heat transfer augmentation and flow characteristics due to rib roughness over absorber plate of a solar air heater, Renew. Energy, 31 (3), 317-331.

Yadav, A. S. and Bhagoria, J. L., 2013a. Modeling and simulation of turbulent flows through a solar air heater having square-sectioned transverse rib roughness on the absorber plate, Sci. world, J.

Yadav, A. S. and Bhagoria, J. L., 2013b. Numerical investigation of flow through an artificially roughened solar heater, Int. J. Ambient Energy.

Yadav, A. S. and Bhagoria, J. L., 2013c. A CFD Based heat transfer and fluid flow analysis of a solar air heater provided with circular transverse wire rib roughness on the absorber plate, Energy, 55, 1127-1142.